Research Journal of Biological Sciences 6 (9): 453-458, 2011
ISSN: 1815-8846

Role of Non-Newtonian Behavior in Blood Flow Through Normal and Stenosed Artery

Sapna Ratan Shah
Department of Mathematics, Harcourt Butler Technological Institute, 208002 Kanpur, India

Abstract: The problem of non-Newtonian blood flow through a stenosed artery is solved numerically where the non-Newtonian rheology of the flowing blood is characterized by the generalized Casson's fluid and Herschel-Bulkley fluid. The necessary theoretical results such as resistance to flow, apparent viscosity and the wall shear stress have been obtained in this analysis. An extensive quantitative analysis is performed through numerical computations of the desired quantities having physiological relevance through their graphical representations so as to validate the applicability of the present model. It has been shown that the resistance to flow, apparent viscosity and wall shear stress increases with the size of the stenosis while decreases as stenosis shape parameter increases. This study shows that non-Newtonian behavior of Herschel-Bulkley fluid model is more appropriate.

Key words: Casson's fluid, Herschel-Bulkley fluid, stenosed arteries, apparent viscosity, resistance to flow, non-Newtonian fluid

INTRODUCTION

The intimal thickening of stenotic artery was understood as an early process in the beginning of atherosclerosis. Atherosclerosis is a leading cause of death in many countries. There is considerable evidence that vascular fluid dynamics plays an important role in development and progression of arterial stenosis which is one of the most widespread diseases in human beings. A Newtonian fluid by definition is one in which the coefficient of viscosity is constant at all rates of shear. Homogeneous liquids may behave closely like Newtonian fluids. However, there are fluids that do not obey the linear relationship between shear stress and shear strain rate. Fluids that exhibit a non-linear relationship between the shear stress and the rate of shear strain are called non-Newtonian fluids. Blood behaviour is referred to as non-Newtonian properties. These properties are of two types as follows; at low shear rates, the apparent viscosity increases markedly-sometimes even a certain yield stress is required for flow; in small tubes, the apparent viscosity at higher rates of shear is smaller than it is in larger tubes. These two types of anomalies are often referred to as low shear and high shear effects, respectively. It is thus concluded that the behaviour of blood is almost Newtonian at high shear rate while at low shear rate the blood exhibits yield stress and non-Newtonian behaviour. In the series of the studies (Casson, 1959; Chakravarty *et al*., 2004; Daripa and Dash, 2002; Fry, 1972), the effects on the cardiovascular system can be understood by studying the blood flow in its vicinity. In these studies the behavior of the blood has been considered as a Newtonian fluid. However, it may be noted that the blood does not behave as a Newtonian fluid under certain conditions. It is generally accepted that the blood, being a suspension of cells, behaves as a non-Newtonian fluid at low shear rate (Haldar, 1985; Hershey *et al*., 1964). It has been pointed out that the flow behaviour of blood in a tube of small diameter (<0.2 mm) and at <20 sec^{-1} shear rate can be represented by a power-low fluid (Jayaraman and Dash, 2001; LaBarbera, 1990). It has also been suggested that at low shear rate (0.1 sec^{-1}), the blood exhibits yield stress and behaves like a Casson-Model fluid. For blood flows in large arterial vessels (i.e., Vessel diameter ≥1 mm) which can be considered as a large deformation flow, the predominant feature of the rheological behavior of blood is its shear rate dependent viscosity and its fact on the hemodynamics of large arterial vessel flows has not been understood well. In this study, researchers investigated the effect of non-Newtonian behavior of blood on the resistance to flow, apparent viscosity and wall shear stress in an artery by considering the blood as Casson's-Model and Herschel-Bulkley fluid and to examine the effect of stenosis shape parameter, researchers considered blood flow through an axially non-symmetrical but radially symmetric stenosis such that the axial shape of the stenosis can be change just by varying a parameter, m.

MATERIALS AND METHODS

Formulation of the problem: In the present analysis, it is assumed that the stenosis develops in the arterial wall

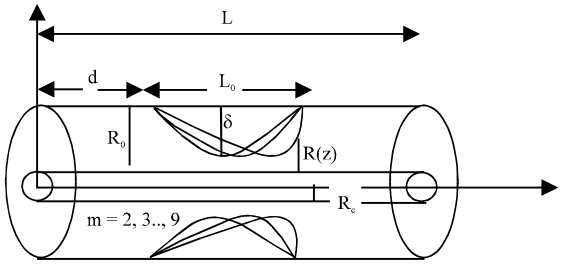

Fig. 1: Flow geometry of an axially non-symmetrical stenosis

in an axially non-symmetric but radially symmetric manner and depends upon the axial distance z and the height of its growth. In such a case, the radius of artery, R(z) can be written as follows (Fig. 1):

$$\left.\begin{aligned}\frac{R(z)}{R_0} &= 1 - A[L_0^{(m-1)}(z-d) - (z-d)^m], \quad d \le z \le d + L_0\\ &= 1 \qquad\qquad\qquad\qquad\qquad \text{otherwise}\end{aligned}\right\} \tag{1}$$

where, R(z) and R_0 is the radius of the artery with and without stenosis, respectively. L_0 is the stenosis length and d indicates its location, $m \ge 2$ is a parameter determining the stenosis shape and is referred to as stenosis shape parameter. Axially symmetric stenosis occurs when m = 2 and a parameter A is given by:

$$A = \frac{\delta}{R_0 L_0^m}\frac{m^{m/(m-1)}}{(m-1)}$$

Where, δ denotes the maximum height of stenosis at $z = d + L_0/m^{1/(m-1)}$.

Conservation equation and boundary condition: The equation of motion for laminar and incompressible, steady, fully-developed, one-dimensional flow of blood whose viscosity varies along the radial direction in an artery reduces to:

$$\begin{aligned}0 &= -\frac{\partial P}{\partial r} + \frac{1}{r}\frac{\partial(r\tau)}{\partial z}\\ 0 &= -\frac{\partial P}{\partial r}\end{aligned} \tag{2}$$

where (z, r) are co-ordinates with z measured along the axis and r measured normal to the axis of the artery. Following boundary conditions are introduced to solve the above equations:

$$\left.\begin{aligned}\partial u/\partial r = 0 \quad & \text{at } r = 0\\ u = 0 \quad & \text{at } r = R(z)\\ \tau \text{ is finite} \quad & \text{at } r = 0\\ P = P_0 \quad & \text{at } z = 0\\ P = P_L \quad & \text{at } z = L\end{aligned}\right\} \tag{3}$$

Case 1; Casson's Fluid Model: The Casson's relation is commonly written as:

$$\left.\begin{aligned}\tau^{1/2} &= \tau_0^{1/2} + (\mu)^{1/2}(-\frac{du}{dr})^{1/2}, \quad \text{if } \tau \ge \tau_0\\ \left(\frac{du}{dr}\right) &= 0 \qquad\qquad\qquad\qquad \text{if } \tau < \tau_0\end{aligned}\right\} \tag{4}$$

$$t_0 = -\frac{dp}{dz}\frac{R_c}{2}$$

Where:

R_c = The radius of the plug-flow region
τ_0 = Yield stress
τ = Wall shear stress
μ = Denotes Casson's viscosity coefficient

The volume rate of flow using Eq.16 is defined as:

$$Q = p\int_0^R r^2(-\frac{du}{dr})dr \tag{5}$$

By integrating Eq. 17, using Eq. 16 and 3 researchers have:

$$Q = \frac{\pi R^4}{8\mu}\left(-\frac{dp}{dz}\right)\left[1 - \frac{16}{7}\left(\frac{R_c}{R}\right)^{1/2} + \frac{4}{3}\left(\frac{R_c}{R}\right) - \frac{1}{21}\left(\frac{R_c}{R}\right)^4\right] \tag{6}$$

Equation 18 can be rewritten as:

$$Q = \frac{\pi R^4}{8\mu}\left(-\frac{dp}{dz}\right)f(\bar{y})$$

Where:

$$f(\bar{y}) = \left[1 - \frac{16}{7}(\bar{y})^{1/2} + \frac{4}{3}(\bar{y}) - \frac{1}{21}(\bar{y})^4\right]$$

With:

$$\bar{y} = \frac{R_c}{R} << 1$$

From above equation pressure gradient is written as follows:

$$\left(-\frac{dp}{dz}\right) = \frac{8\mu Q}{\pi R^4 f(\bar{y})} \tag{7}$$

Integrating Eq. 19 using the condition $P = P_0$ at $z = 0$ and $P = P_L$ at $z = L$. Researchers have:

$$\Delta P = P_L - P_0 = \frac{8\mu Q}{\pi R_0^4}\int_0^L \frac{dz}{\left(R(z)/R_0\right)^4 f\left(\bar{y}(z)\right)} \tag{8}$$

The resistance to flow (resistive impedance) is denoted by λ and defined as follows:

$$\lambda = \frac{P_L - P_0}{Q} \tag{9}$$

The resistance to flow from Eq. 21 using Eq. 20 is written as:

$$\lambda = 1 - \frac{L_0}{L} + \frac{f_0}{L}\int_d^{d+L_0} \frac{dz}{\left(R(z)/R_0\right)^4 f\left(\bar{y}(z)\right)} \tag{10}$$

where, f_0 is given by:

$$f_0 = \left[1 - \frac{16}{7}\left(\frac{R_c}{R_0}\right)^{1/2} + \frac{4}{3}\left(\frac{R_c}{R_0}\right) - \frac{1}{21}\left(\frac{R_c}{R_0}\right)^4\right]$$

Following the apparent viscosity (μ_{app}) is defined as follows:

$$\mu_{app} = \frac{1}{\left(R(z)/R_0\right)^4 f\left(\bar{y}\right)} \tag{11}$$

The shearing stress at the wall can be defined as:

$$\tau_R = \left[\tau_0^{1/2} + \left(-\mu\frac{du}{dr}\right)_{r=R(z)}^{1/2}\right]^2 \tag{12}$$

Case 2; Herschel-Bulkley Fluid Model: The stress-strain relation of Herschel-Bulkley fluid is given as:

$$\begin{aligned} f(\tau) &= \left(-\frac{du}{dr}\right) = \frac{1}{\mu}(\tau - \tau_0)^n, \quad \tau \geq \tau_0 \\ f(\tau) &= \left(-\frac{du}{dr}\right) = 0, \qquad\qquad \tau \leq \tau_0 \end{aligned} \tag{13}$$

Where:

$$\tau = \left(-\frac{dp}{dz}\frac{r}{2}\right)$$

$$\tau_0 = \left(-\frac{dp}{dz}\frac{R_c}{2}\right)$$

μ = Denotes Herschel-Bulkley viscosity coefficient
τ_o = Yield stress
τ = Shear stress
R_c = The radius of the plug-flow region
u = The axial velocity along the z direction
n = The flow behavior index

The relation correspond to the vanishing of the velocity gradients in regions in which the shear stress τ is less than the yield stress τ_o this implies a plug flow wherever $\tau \leq \tau_o$ when the shear rates in the fluid are very high, $\tau \geq \tau_o$, the power-law fluid behavior is indicated. By Eq. 1 and 3 researchers get:

$$\left(\frac{du}{dr}\right) = -\left(\frac{p}{2\mu}\right)^{1/n}\left[\left(r - R_c\right)^{1/n}\right] \tag{14}$$

The flow of flux, Q is defined as:

$$Q = \int_0^R 2\,p\,u\,r\,dr = p\int_0^R r^2\left(-\left(du/dr\right)\right)dr \tag{15}$$

Substituting the value of $f(\tau)$ from Eq. 1 in Eq. 7:

$$Q = \frac{\pi}{2}\left(\frac{P}{2\mu}\right)^{1/n}\frac{R^{\left(3+\frac{1}{n}\right)}}{\left(1+\frac{1}{n}\right)}f(y) \tag{16}$$

$$f(y) = \left[\begin{array}{l} 2\left(1-\frac{R_c}{R}\right)^{((1/n)+1)} - \frac{4}{\left((1/n)+2\right)}\left(1-\frac{R_c}{R}\right)^{((1/n)+2)} \\ + \frac{4}{\left((1/n)+2\right)\left((1/n)+3\right)}\left(\left(1-\frac{R_c}{R}\right)^{((1/n)+3)}\right) - \\ \left(\left(\left(-1\right)^{((1/n)+3)}\left(\frac{R_c}{R}\right)\right)\right) \end{array}\right]$$

where:

$$\bar{y} = (R_c/R) << 1$$

Using Eq. 8 researchers have:

$$P = \left(-\frac{dp}{dz}\right) = \frac{2\mu}{R^{(1+3n)}}\left(\frac{2Q}{\pi f(\bar{y})}(1+\frac{1}{n})\right)^n \tag{17}$$

to determine λ, researchers integrate Eq. 11 for the pressure P_L and P_o are the pressure at $z = 0$ and $z = L$, respectively where L is the length of the tube:

$$\Delta P = P_L - P_0 = \frac{2\mu}{\pi R_0^{1+3n}}\left(2Q\left(\frac{1}{n}+1\right)\right)^n \int_0^L \frac{dz}{\left(R(z)/R_0\right)^{(1+3n)}\left(f(\bar{y})\right)^n} \tag{18}$$

The resistance to flow is given by the coefficient λ is defined as follows:

$$\lambda = (P_L - P_0/Q) \tag{19}$$

$$\lambda_0 = \frac{2\mu}{R_0^{1+3n}}\left(\frac{2Q(1+\frac{1}{n})}{\pi}\right)^n (M)$$

$$M = \left(\int_0^d \frac{dz}{(f_0)^n} + \int_d^{d+L_0} \frac{dz}{\left(\frac{R(z)}{R_0}\right)^{1+3n}(f(\bar{y}))^n} + \int_{d+L_0}^{L} \frac{dz}{(f_0)^n}\right)$$

$$f_0 = \left[2(1-\bar{y}_1)^{\left(1+\frac{1}{n}\right)} - \frac{4}{\left(\frac{1}{n}+2\right)}(1-\bar{y}_1)^{\left(2+\frac{1}{n}\right)} + \frac{4}{\left(2+\frac{1}{n}\right)\left(3+\frac{1}{n}\right)}\left((1-\bar{y}_1)^{\left(3+\frac{1}{n}\right)} - \left((-1)^{\left(3+\frac{1}{n}\right)}\bar{y}_1\right)\right)\right] \tag{20}$$

Where:

$$\bar{y}_1 = (R_c/R_0)$$

When there is no stenosis in artery then R = R_0, the resistance to flow:

$$\lambda_N = \frac{2\mu}{R_0^{1+3n}}\left(\frac{2Q\left(1+\frac{1}{n}\right)}{\pi}\right)^n \frac{L}{(f_0)^n} \tag{21}$$

from Eq. 12 and 13 the ratio of (λ/λN) is given as:

$$\lambda = \frac{\lambda_0}{\lambda_N} = 1 - \frac{L_0}{L} + \frac{(f_0)^n}{L}\int_d^{d+L_0} \frac{dz}{(R(z)/R_0)^{1+3n} f(\bar{y})^n} \tag{22}$$

The apparent viscosity (μ_0/μ) is defined as follow:

$$\mu_{app} = (1/(R(z)/R_0)^{1+3n} f(\bar{y}))$$

Figure 2 shows the variation of resistance to flow (λ) with stenosis shape parameter (m) for stenosis size (δ/R_0). It is seen from Fig. 2 that the resistance to flow decreases as stenosis shape parameter increases. Maximum resistance to flow occurs at m = 2, i e., in the case of symmetric stenosis. This result is therefore consistent with the observation of Mishra *et al.* (2010). Figure 3 shows the variation of resistance to flow with stenosis length for different values of stenosis shape parameter. Figure 3 shows that resistance to flow increases as stenosis length increases and decreases as stenosis shape parameter increases. This result is qualitative agreement with the observation of Neofytou and Drikakis (2003).

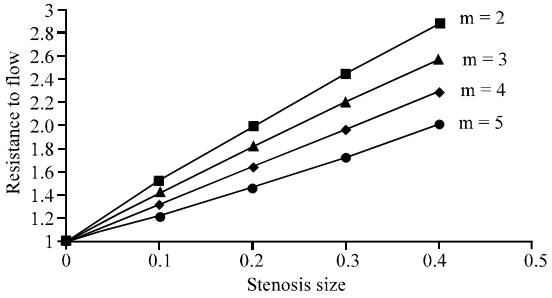

Fig. 2: Variation of resistance to flow with stenosis size (n = 1)

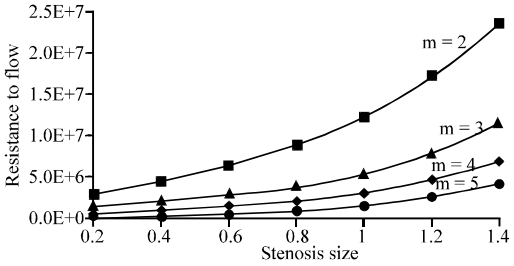

Fig. 3: Variation of resistance to flow with stenosis size (n = 2/3)

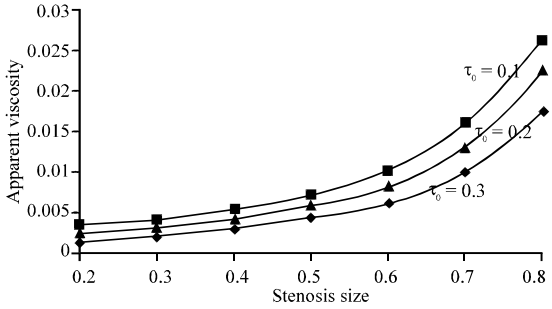

Fig. 4: Variation of apparent viscosity with stenosis size (n = 2/3)

Figure 4 shows variation of apparent viscosity with Stenosis shape parameter. Figure 4 shows that apparent viscosity decreases as stenosis shape parameter increases but this increase is less due to non-Newtonian behaviour of the blood. In addition, it may be noted from the graph that the apparent viscosity increases as stenosis size increases. This result is in qualitative agreement with the result of Ookawara and Ogowa (2000) and Pontrelli (2001). It may be observed that

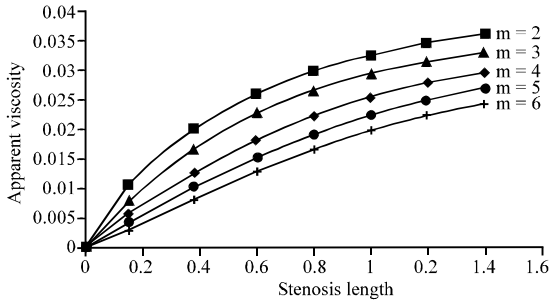

Fig. 5: Variation of apparent viscosity with stenosis length (n = 1/3)

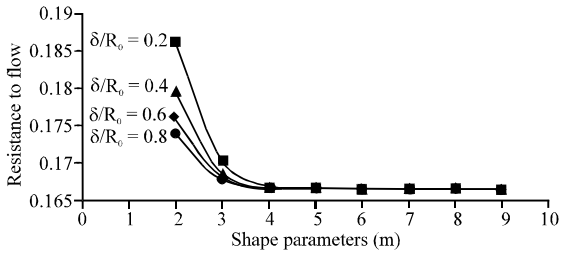

Fig. 6: Variation of resistance to flow with shape m for stenosis

from these results that the apparent viscosity increases as the stenosis grows and remains constants outside from the stenotic region. Figure 5 shows the variation of apparent viscosity with stenosis length for different values of stenosis shape parameter. Researchers observe that the apparent viscosity sharply increases as length of stenosis increases and decreases as stenosis shape parameter increases.

Rachid and Ouazzani (2008) and Sankar and Hemalatha (2006) have also noted the same results. Figure 6 consist the variation of resistance to flow with stenosis shape parameter for different values of stenosis size. It is observed here that the resistance to flow decreases as the stenosis shape parameter increases. It should also be noted here that the resistance to flow decreases as stenosis size increases.

The results are therefore consistent with the observation of Shalmanab *et al.* (2009) and Shukla *et al.* (1980). Figure 7 shows the variation of resistance to flow with stenosis length for different values of stenosis shape parameter. In Fig. 7, resistance to flow increases as stenosis length increases. It is also noticed here that resistance to flow decreases as stenosis shape parameter increases for fixed value of stenosis size. This result is obvious because the lumen radius decreases as stenosis size increases (Srivastava and Mishra, 2010). Figure 8 shows the variation of resistance to flow with yield stress

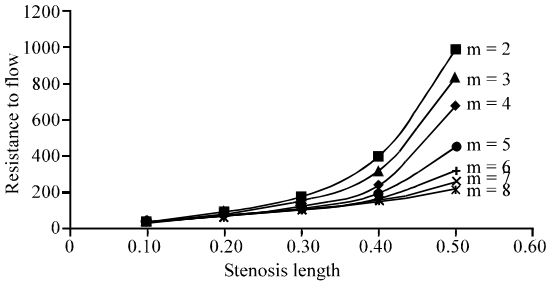

Fig. 7: Variation of resistance to flow with stenosis length

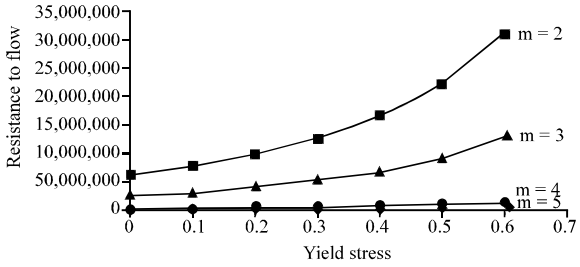

Fig. 8: Variation of resistance to flow with yield stress

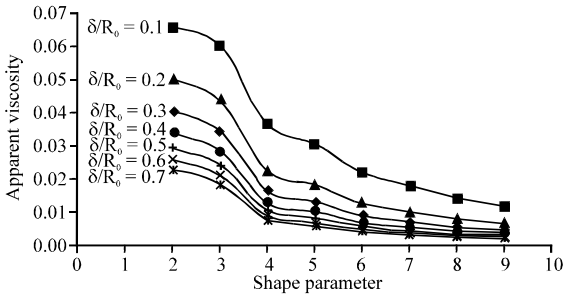

Fig. 9: Variation of apparent viscosity with stenosis shape parameter for different values of stenosis size

for different values of stenosis shape parameter. It is evident from the graph that the resistance to flow increases as yield stress increases. Figure 8 is also highlighted that resistance to flow decreases as stenosis shape parameter increases (Tandon *et al.*, 1991; Tang *et al.*, 2000). Figure 9 shows the variation of apparent viscosity with stenosis shape parameter for different values of stenosis size. It may be observed here that the apparent viscosity decreases as shape parameter of stenosis varies. Figure 9 is also depicted that apparent viscosity decreases as stenosis size increases.

CONCLUSION

In this study, researchers have studied the effects of the stenosis in an artery by considering the blood as

Casson's Fluid and Herscel-Bulkley Fluid Models. It has been concluded that the resistance to flow and wall shear stress increases as the size of stenosis increases for a given non-Newtonian Model of the blood. The flow resistance decreases with increasing values of shape parameter 'm' and attains its maximal in the symmetric stenosis case (m = 2) for any given stenosis size. Thus the increasing value of the shape parameter would cause a considerable increase in the flow of blood. These increases are however small due to non-Newtonian behaviour of the blood. Thus, it appears that the non-Newtonian behaviour of the blood is helpful in the functioning of diseased arterial circulation.

REFERENCES

Casson, N., 1959. A Flow Equation for Pigment Oil Suspensions of the Printing Ink Type. In: Rheology of Disperse Systems, Mill, C.C. (Ed.). Pergamon Press, London, Pp: 84-102.

Chakravarty, S., Sharifuddinn and P.K. Mandal, 2004. Unsteady flow of a two-layer blood stream past a tapered flexible artery under stenotic conditions. Comput. Met. Appl. Math, 4: 391-409.

Daripa, P. and R.K. Dash, 2002. A numerical study of pulsatile blood flow in an eccentric catheterized artery using a fast algorithm. J. Eng. Math., 42: 1-22.

Fry, D.L., 1972. Localizing Factor In Arteriosclerosis, In atherosclerosis and Coronary Heart Disease. Grune Stratton, NewYork, Pages: 85.

Haldar, K., 1985. Effects of the shape of stenosis on the resistance to blood flow through an arter. Bull. Math. Biol., 47: 545-550.

Hershey, D., R.E. Byrnes, R.L. Deddens and A.M. Roa, 1964. Blood rheology: Temperature dependence of the power law model. Paper Presented at A.I.Ch.E. Boston.

Jayaraman, G. and Dash R.K., 2001. Numerical study of flow in a constricted curved annulus: An application to flow in a catheterized artery. J. Eng. Math., 40: 355-375.

LaBarbera, M., 1990. Principles of design of fluid transport systems in zoology. Science, 249: 992-1000.

Mishra, B.K., P. Pradhan and T.C. Panda, 2010. Effect of shear stress, resistance and flow rate across mild stenosis on blood flow through blood vessels. The Cardiol., 5: 4-11.

Neofytou, P. and D. Drikakis, 2003. Non-Newtonian flow in instability in a channel with a sudden expansion. J. Non-Newtonian Fluid Mech., 11: 127-150.

Ookawara, S. and K. Ogowa, 2000. Flow properties of Newtonian and non Newtonian fluid downstream of stenosis. J. Chem. Engg. Jap., 33: 582-590.

Pontrelli, G., 2001. Blood flow through an axisymmetric stenosis. Proc. Inst. Mech. Eng. H, 215: 1-10.

Rachid, H. and M.T. Ouazzani, 2008. The effect of pulsatile flow on peristaltic output: Case of a Newtonian fluid. Stud. Theor. Phys., 6: 29-30.

Sankar, D.S. and K. Hemalatha, 2006. Pulsatile flow of herschel-bulkey fluid through stenosed arteries: A mathematical model. Int. J. Non-Liner Mech., 41: 979-990.

Shalmanab, E., M. Rosenfelda, E. Dganyb and S. Einava, 2009. Numerical modeling of the flow in stenosed coronary artery. Relat. Between Main Hemodynamic Parameters, 12: 589-602.

Shukla, J.B., S.P. Gupta and R.S. Parihar, 1980. Biorheological aspects of blood flow through artery with mild stenosis: Effects of peripheral layer. Biorheology, 17: 403-410.

Srivastava, V.P. and S. Mishra, 2010. Non-Newtonian arterial blood flow through an overlapping stenosis. Appl. Applied Math., 5: 225-238.

Tandon, P.N., P. Nirmala, M. Tewari and U.S. Rana, 1991. Analysis of nutritional transport through a capillary: Normal and stenosed. Comput. Math. Appl., 22: 3-13.

Tang, D., C. Yang, H. Walker, S. Kobayashi and D.N. Ku, 2000. Simulating cyclic artery compression using a 3-D unsteady model with fluid-structure interactions. Comput. Struct., 80: 1651-1665.